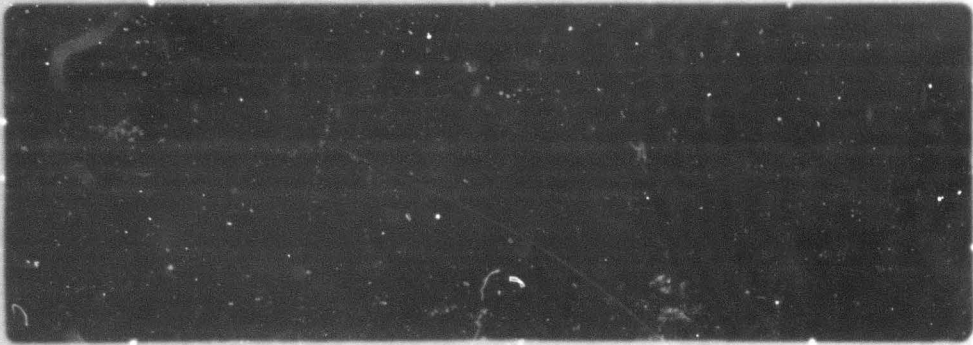


601616

293

32 ps - \$1.00



**PHILCO.**

A SUBSIDIARY OF *Ford Motor Company,*  
AERONUTRONIC DIVISION

**PHILCO**

A SUBSIDIARY OF *Ford Motor Company*  
AERONUTRONIC DIVISION

Publication No. U-2630

**RE-ENTRY AND SPACE SYSTEMS PROGRAMS**

---

**ENGINEERING ANALYSIS TECHNICAL NOTE NO. 24**

---

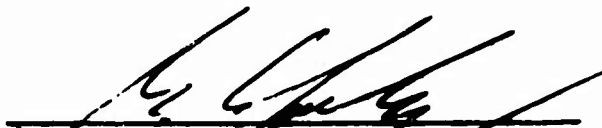
**AN APPROXIMATE METHOD FOR CALCULATING  
THE FLOW FIELD OF A ROCKET EXHAUSTING INTO A VACUUM**

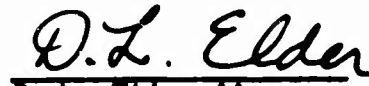
Prepared for: Ballistic Systems Division  
United States Air Force  
Norton Air Force Base, California

Under Contract: AF 04(694)-23

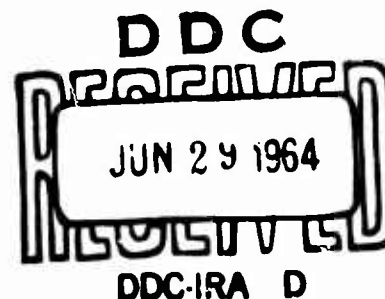
Prepared by: A. I. Karydas and H. T. Kato, Engineering Analysis

Approved by:

  
G. A. Lasky, Program Manager  
Air Force Penetration Aids  
Re-entry and Space Systems Programs

  
D. L. Elder, Manager  
Engineering Analysis

15 June 1964



## CONTENTS

SECTION	PAGE
1 INTRODUCTION . . . . .	1
2 ANALYSIS . . . . .	2
3 RESULTS AND DISCUSSION . . . . .	10
REFERENCES . . . . .	12
APPENDIX EXAMPLE CALCULATIONS . . . . .	13
FIGURES . . . . .	16
DISTRIBUTION. . . . .	25

### ILLUSTRATIONS

FIGURE	PAGE
1 Theoretical Streamlines for a Nozzle Exhausting Into a Vacuum Compared With Streamlines for Radial Flow From a Point Source . . .	16
2 Jet Geometry and Coordinate System . . . . .	17
3 Contours of Constant Mach Number for a Rocket Exhausting Into a Vacuum (by Present Approximate Solution) . . . . .	18
4a Sonic Nozzle Flow Field in a Vacuum ( $M_e = 1.0$ , $\gamma = 1.4$ ) . . . . .	19
4b Mach Number Transformation Curves ( $\gamma = 1.4$ ) . . . . .	20
5 A Comparison of the Approximate and Characteristics Solutions for a Rocket Exhausting Into a Vacuum ( $M_e = 2.94$ , $\gamma = 1.4$ ) . . . . .	21
6 Comparison of Axial Mach Number Distribution for a Rocket Exhausting Into a Vacuum ( $M_e = 1.0$ , $\gamma = 1.4$ ) . . . . .	22
7 A Comparison of the Approximate and Characteristics Solutions for a Rocket Exhausting Into a Vacuum ( $M_e = 3.93$ , $\gamma = 1.26$ ) . . . . .	23
8 A Comparison of the Approximate and Characteristics Solution for a Rocket Exhausting Into a Vacuum ( $M_e = 4.0$ , $\gamma = 1.24$ ) . . . . .	24

## SUMMARY

An approximate method for determining the far field flow properties of a rocket exhausting into a vacuum is presented. The technique described is based on radial flow and assumes a density variation both along and normal to the jet centerline. The resulting jet flow field is compared with solutions by the method of characteristics and is shown to have good agreement. Example calculations are provided to demonstrate the present method.

## NOMENCLATURE

<b>a</b>	Speed of sound
<b>A</b>	Area
<b>E</b>	Constant defined by Equation (13)
<b>E'</b>	Constant defined by Equation (26)
<b>h</b>	Radius from nozzle exit
<b>M</b>	Local Mach number at the point $(h, \theta)$
<b>M'</b>	Local Mach number at the point $(h, \theta)$ in the flow field of a sonic nozzle
<b>N</b>	Constant defined in Equation (4)
<b>P</b>	Pressure
<b>r</b>	Radius
<b>S</b>	Control surface
<b>V</b>	Velocity
<b>X</b>	Axial distance from nozzle exit
<b>Y</b>	Distance normal to jet centerline
<b><math>\gamma</math></b>	Gas ratio of specific heats
<b><math>\rho</math></b>	Gas density

### Subscripts

<b>e</b>	Nozzle exit conditions
<b>*</b>	Nozzle throat conditions
<b>o</b>	Stagnation (chamber) conditions
<b>s</b>	Refers to spherical cap

## OBJECTIVES

The objective of this technical note is to describe an approximate method for determining the far field flow properties for a rocket exhausting into a vacuum.

## CONCLUSIONS AND RECOMMENDATIONS

An approximate method for determining the far field flow properties for a rocket exhausting into a vacuum has been presented. A comparison of Mach number distribution both along and normal to the jet axis with solutions by the method of characteristics indicates good agreement. The present method should provide an adequate approximation for rocket flow field problems in a vacuum. Recommendations are the following:

- (1) Investigate further the limits of this approximate solution for:
  - (a) Nonvacuum conditions.
  - (b) Nozzles with noncircular cross sections at the exit plane.
- (2) Develop an improved approximate method which describes the exhaust flow past 90 degrees. (The present method is limited to expansion angles less than 90 degrees.)

## SECTION 1

### INTRODUCTION

When a rocket exhausts into a vacuum, the flow undergoes a large expansion and the resulting free jet of gas occupies a considerable volume in space. The presence of this large free jet of gas can produce serious aerodynamic, aerothermal, and communications problems. Some of these problems are: the effects of jet impingement forces on the dynamics of nearby surfaces; the exhaust blast on the surface of the moon during ascent or descent of a rocket; the heating of nearby surfaces submerged in the rocket plume; and the effects of the exhaust gas on visual or other guidance information.

In order to investigate these problems, an adequate definition of the rocket exhaust flow field is necessary. In most cases, the method of characteristics has been utilized to determine properties in the rocket flow field. However, the procedure is quite laborious, costly, and generally requires machine computations. To provide a more convenient and practicable means for defining the rocket flow field in a vacuum, an approximate method is described in this technical note. The technique can be utilized to calculate pressures, densities, temperatures and Mach numbers in the rocket flow field from a knowledge of only the nozzle geometry and the ratio of specific heats for the gas.

## SECTION 2

### ANALYSIS

Consider the exhaust jet of an ideal inviscid gas issuing isentropically from a nearly parallel nozzle (of exit radius  $r_e$  and exit Mach number  $M_e$ ) into a vacuum. The flow is continuous and steady, and the ratio of specific heats,  $\gamma$ , is assumed constant.

At distances large compared to the nozzle dimensions, theoretical solutions for the exhaust flow in a vacuum show that the flow field approaches radial flow, i.e., the streamlines are straight and appear to emanate from a common source (see Figure 1). The basic solution of radial flow stipulates that the mass flux,  $\rho V$ , varies as  $1/h^2$ , where  $h$  is the radial distance from the nozzle. In a vacuum, the pressure rapidly approaches zero so that the velocity can be assumed constant. In this case, the density takes the form  $\rho \sim 1/h^2$ .

Most of the mass and momentum of the jet are concentrated near the jet centerline, so that the variation of density in the direction normal to the jet centerline must be considered. Reference 1 assumes that the density on a spherical cap at a distance  $h$  from the nozzle exit is of the form:

$$\frac{\rho}{\rho_e} = B \left( \frac{h}{r_e} \right)^{-2} (\cos \theta)^K \quad (1)$$

where  $\theta$  is the azimuthal angle measured from the jet centerline, and  $B$  and  $K$  are constants. By integrating the conservation of mass and momentum equations, and neglecting terms of order  $1/M_e^2$ , Reference 1 has obtained a first-order solution for the density profile:

$$\frac{\rho}{\rho_e} = \frac{K}{2} \left( \frac{h}{r_e} \right)^{-2} (\cos \theta)^K \quad (2)$$



where  $K = \gamma (\gamma - 1) M_e^2$ . The above expression has the restriction that  $M_e^2 \gg 1$  and  $\frac{h}{r_e} \gg 1$ .

In the present analysis, a more general solution which includes the effects of higher order terms is sought, i.e., it is desirable to remove the restriction in Equation (2) that  $M_e^2 \gg 1$ . The basic approach to the problem is that of Reference 1. A density profile similar in form to Equation (1) is assumed. The continuity and momentum equations are then solved simultaneously to obtain the density distribution in the jet flow field. From this result, a generalized method for calculating contours of constant Mach number for a rocket flow field in a vacuum is derived.

The system under analysis is shown in Figure 2 (a) and (b). The flow is considered radial and axially symmetric. The surface  $S$  is the sum of the hemispherical surface ( $A_s$ ) of radius  $h$ , and its projection on the  $Y-Z$  plane,  $A_{Y-Z}$ . Flow enters the control surface only through the nozzle exit area,  $A_e$ , and exits through the surface,  $A_s$ .

On the spherical cap, the velocity is assumed radial and constant. That is,\*

$$\mathbf{V}_s = V_{\max} \mathbf{n} \quad (3)$$

where  $V_{\max}$  is the maximum velocity obtainable by expanding to zero pressure, and  $\mathbf{n}$  is a unit vector\* everywhere normal to the surface  $S$ . The density profile on the surface,  $A_s$ , is assumed to be of the form:

$$\frac{\rho}{\rho_e} = \frac{E}{2} \left( \frac{V_e}{V_{\max}} \right) \left( \frac{h}{r_e} \right)^{-2} (\cos \theta)^N \quad (4)$$

where  $E$  and  $N$  are constants.

For steady flow, the integral form of the continuity equation is:

$$\oint_S \rho (\mathbf{V} \cdot \mathbf{n}) dS = 0$$

Over the surface  $S$  (see Figure 2), the above integral is written:

$$\iint_{A_s} \rho (\mathbf{V}_s \cdot \mathbf{n}) dA_s - (\rho_e V_e A_e) = 0 \quad (5)$$

Introducing the expressions for  $\mathbf{V}_s$  from Equation (3) and  $\rho$  from Equation (4), then

\*Vector quantities are symbolized by bold-face letters.

Equation (5) becomes:

$$\int_0^{\pi/2} \left[ \rho_e \frac{E}{2} \left( \frac{v_e}{v_{\max}} \right) \left( \frac{h}{r_e} \right)^{-2} (\cos \theta)^N \right] \left[ v_{\max} \mathbf{n} \cdot \mathbf{n} \right] \left[ 2 \pi h^2 \sin \theta \right] d\theta = \rho_e v_e A_e \quad (6)$$

Integrating and solving for E, we obtain:

$$E = N+1 \quad (\text{continuity}) \quad (7)$$

Conservation of momentum need be considered only in the X-direction, since the flow is axially symmetric. The integral form of the conservation of momentum equation in the X-direction is:

$$\oint_S \rho (\mathbf{V} \cdot \mathbf{n}) dS (\mathbf{V} \cdot \mathbf{i}) + \oint_S p (\mathbf{n} \cdot \mathbf{i}) dS = 0$$

For the surface S, the above integral becomes:

$$\iint_{A_s} \left[ \rho (\mathbf{V}_s \cdot \mathbf{n}) (\mathbf{V}_s \cdot \mathbf{i}) + p (\mathbf{n} \cdot \mathbf{i}) \right] dA_s = \left( \rho_e v_e^2 + p_e \right) A_e \quad (8)$$

Substitution of the expressions for  $\mathbf{V}_s$  and  $\rho$  (from Equations (3) and (4) respectively) into Equation (8) results in the integral:

$$\begin{aligned} \int_0^{\pi/2} \left[ \rho_e \frac{E}{2} \left( \frac{v_e}{v_{\max}} \right) \left( \frac{h}{r_e} \right)^{-2} (\cos \theta)^N \right] \left[ v_{\max} \mathbf{n} \cdot \mathbf{n} \right] \left[ v_{\max} \mathbf{n} \cdot \mathbf{i} \right] \left[ 2 \pi h^2 \sin \theta \right] d\theta \\ = \left( \rho_e v_e^2 + p_e \right) A_e \\ = \rho_e v_e^2 \left( 1 + \frac{1}{\gamma M_e^2} \right) A_e \end{aligned} \quad (9)$$

Solving Equation (9) for E, we obtain:

$$E = (N + 2) \left( \frac{v_e}{v_{\max}} \right) \left( 1 + \frac{1}{\gamma M_e^2} \right) \quad (\text{momentum}) \quad (10)$$

The constant E can now be determined by solving Equations (7) and (10)

simultaneously. Thus,

$$E = \frac{\left(\frac{V_e}{V_{\max}}\right) \left(1 + \frac{1}{\gamma M_e^2}\right)}{1 - \left(\frac{V_e}{V_{\max}}\right) \left(1 + \frac{1}{\gamma M_e^2}\right)} \quad (11)$$

The velocity ratio,  $(V_e/V_{\max})$ , is related to the nozzle exit Mach number,  $M_e$ , by the adiabatic relationship

$$\frac{V_e}{V_{\max}} = \frac{1}{\sqrt{1 + \frac{2}{(\gamma - 1)M_e^2}}} \quad (12)$$

Then, Equation (11) becomes:

$$E = \frac{1 + \frac{1}{\gamma M_e^2}}{\sqrt{1 + \frac{2}{(\gamma - 1)M_e^2}} - \left(1 + \frac{1}{\gamma M_e^2}\right)} \quad (13)$$

Substituting Equation (7) into Equation (4), the density distribution in the flow field is obtained

$$\frac{\rho}{\rho_e} = \frac{E}{2} \left(\frac{V_e}{V_{\max}}\right) \left(\frac{h}{r_e}\right)^{-2} (\cos \theta)^{(E-1)} \quad (14)$$

where  $E$  is defined by Equation (13) and  $(V_e/V_{\max})$  by Equation (12). It is seen that both  $E$  and  $(V_e/V_{\max})$  are functions of only  $M_e$  and the ratio of specific heats,  $\gamma$ . Thus, for a given gas and nozzle exit Mach number,  $M_e$ , the density depends only on the location in the flow field  $(h, \theta)$ .

Assuming that the flow inside of the nozzle is isentropic, the Mach number distribution in the flow field can be derived from the isentropic relationship between density and Mach number.

That is,

$$\frac{\rho}{\rho_o} = \left[ 1 + \frac{\gamma-1}{2} M^2 \right]^{\frac{1}{1-\gamma}} \quad (15)$$

where  $\rho_o$  is the stagnation (chamber) density.

Solving the above expression for the Mach number, we obtain

$$M = \left\{ \frac{2}{\gamma-1} \left[ \left( \frac{\rho}{\rho_o} \right)^{1-\gamma} - 1 \right] \right\}^{1/2} \quad (16)$$

The density ratio,  $\frac{\rho}{\rho_o}$ , can be expressed

$$\frac{\rho}{\rho_o} = \frac{\rho}{\rho_e} \cdot \frac{\rho_e}{\rho_o} \quad (17)$$

Substituting Equation (14) into Equation (17), then

$$\frac{\rho}{\rho_o} = \frac{E}{2} \left( \frac{v_e}{v_{\max}} \right) \left( \frac{h}{r_e} \right)^{-2} (\cos \theta)^{(E-1)} \cdot \frac{\rho_e}{\rho_o} \quad (18)$$

From continuity considerations,

$$\rho_e v_e = \rho_{*} a_{*} \left( \frac{A_{*}}{A_e} \right) \quad (19)$$

Thus, Equation (18) becomes:

$$\frac{\rho}{\rho_o} = \frac{E}{2} \left( \frac{h}{r_e} \right)^{-2} (\cos \theta)^{(E-1)} \frac{\rho_{*} a_{*}}{\rho_o v_{\max}} \left( \frac{A_{*}}{A_e} \right) \quad (20)$$

Introducing the isentropic relationships,

$$\frac{\rho_{*}}{\rho_o} = \left( \frac{\gamma+1}{2} \right)^{\frac{1}{1-\gamma}} \quad (21)$$

and

$$\frac{a_*}{V_{\max}} = \left( \frac{\gamma-1}{\gamma+1} \right)^{1/2} \quad (22)$$

Then Equation (20) is written:

$$\frac{\rho}{\rho_0} = \frac{E}{2} \left( \frac{h}{r_e} \right)^{-2} (\cos \theta)^{(E-1)} \left( \frac{A_*}{A_e} \right) \left( \frac{\gamma+1}{2} \right)^{\frac{1}{1-\gamma}} \left( \frac{\gamma-1}{\gamma+1} \right)^{1/2} \quad (23)$$

Combining Equation (23) with Equation (16), the final form for the Mach number is obtained:

$$M = \left[ \frac{2}{\gamma-1} \left\{ \frac{E}{2} \left( \frac{A_*}{A_e} \right) \left( \frac{h}{r_e} \right)^{-2} (\cos \theta)^{(E-1)} \left( \frac{\gamma+1}{2} \right)^{\frac{1}{1-\gamma}} \left( \frac{\gamma-1}{\gamma+1} \right)^{1/2} \right\}^{1-\gamma} - 1 \right]^{1/2} \quad (24)$$

where E is given by Equation (13).

Significant to note, for a given gas and nozzle geometry, the Mach number depends only on the location in the flow field ( $h, \theta$ ). The above expression, Equation (24) is general and can be used to find local Mach numbers in the flow field for any specified  $M_e$  and  $\gamma$ . The main restriction, implied in the radial flow assumption, is that  $\frac{h}{r_e} \gg 1$ .

Equation (24) has been applied to construct contours of constant Mach numbers in Figure 3 for  $M_e = 2.21$  and  $\gamma = 1.24$ . Axial distances from the nozzle exit are given by X and distances normal to the jet centerline by Y. Evidently  $h^2 = X^2 + Y^2$ , and  $\theta = \tan^{-1} Y/X$ . The distances X and Y are normalized by the nozzle exit radius,  $r_e$ . A numerical example of Equation (24) is also provided in the Appendix, Example 1.

Examination of Equation (24) suggests that for each set of  $M_e$  and  $\gamma$ , a separate Mach number chart like Figure 3 must be constructed. For many variations in  $M_e$  and  $\gamma$ , the computations become quite excessive. However, by considering a specified gas ( $\gamma$  fixed), a mathematical simplification of Equation (24) is possible. Let  $M'$  designate the local Mach number at the point ( $h, \theta$ ) in the flow field of a sonic nozzle ( $M_e = 1.0$ ); and,  $M$ , the local Mach number at the same point ( $h, \theta$ ) in the flow field of a nozzle with an exit Mach number,  $M_e$ , other than one. The ratio of specific heats,  $\gamma$ , is the same for both cases.

For a sonic nozzle,  $M_e = 1.0$ ,  $r_e = r_*$ , and, hence,  $\frac{A_*}{A_e} = 1$ .

Substitution of these terms into Equation (24) results in:

$$M' = \left[ \frac{2}{\gamma-1} \left\{ \left[ \frac{E'}{2} \left( \frac{h}{r_*} \right)^{-2} (\cos \theta)^{(E'-1)} \left( \frac{\gamma+1}{2} \right)^{\frac{1}{1-\gamma}} \left( \frac{\gamma-1}{\gamma+1} \right)^{1/2} \right]^{1-\gamma} - 1 \right\} \right]^{1/2} \quad (25)$$

where

$$E' = (\gamma^2 - 1) + \gamma \sqrt{\gamma^2 - 1} \quad (26)$$

In the general case, for a nozzle exit Mach number other than one, the local Mach number,  $M$ , is given directly by Equation (24). Combining Equations (25) and (24),

$$\frac{M}{M'} = \frac{\left\{ \frac{E}{2} \left( \frac{A_*}{A_e} \right) \left( \frac{h}{r_e} \right)^{-2} (\cos \theta)^{(E-1)} \left( \frac{\gamma+1}{2} \right)^{\frac{1}{1-\gamma}} \left( \frac{\gamma-1}{\gamma+1} \right)^{1/2} \right\}^{1-\gamma} - 1 \right\}^{1/2}}{\left\{ \frac{E'}{2} \left( \frac{h}{r_*} \right)^{-2} (\cos \theta)^{(E'-1)} \left( \frac{\gamma+1}{2} \right)^{\frac{1}{1-\gamma}} \left( \frac{\gamma-1}{\gamma+1} \right)^{1/2} \right\}^{1-\gamma} - 1 \right\}^{1/2}} \quad (27)$$

For  $\frac{h}{r_e} \gg 1$ , the terms of the left hand side of the numerator of Equation (27) are large compared to unity. That is,

$$\left\{ \frac{E}{2} \left( \frac{A_*}{A_e} \right) \left( \frac{h}{r_e} \right)^{-2} (\cos \theta)^{(E-1)} \left( \frac{\gamma+1}{2} \right)^{\frac{1}{1-\gamma}} \left( \frac{\gamma-1}{\gamma+1} \right)^{1/2} \right\}^{1-\gamma} - 1 \approx \left\{ \frac{E}{2} \left( \frac{A_*}{A_e} \right) \left( \frac{h}{r_e} \right)^{-2} (\cos \theta)^{(E-1)} \left( \frac{\gamma+1}{2} \right)^{\frac{1}{1-\gamma}} \left( \frac{\gamma-1}{\gamma+1} \right)^{1/2} \right\}^{1-\gamma} \quad (28)$$

Since  $\frac{h}{r_*} = \frac{h}{r_e} \sqrt{\frac{A_e}{A_*}}$ , then  $\frac{h}{r_*} > \frac{h}{r_e} \gg 1$ .

By a similar argument, the denominator of Equation (27) can be written:

$$\left\{ \left[ \frac{E'}{2} \left( \frac{h}{r_*} \right)^{-2} (\cos \theta)^{(E'-1)} \left( \frac{\gamma+1}{2} \right)^{\frac{1}{1-\gamma}} \left( \frac{\gamma-1}{\gamma+1} \right)^{1/2} \right]^{1-\gamma} - 1 \right\} \approx \left[ \frac{E'}{2} \left( \frac{h}{r_*} \right)^{-2} (\cos \theta)^{(E'-1)} \left( \frac{\gamma+1}{2} \right)^{\frac{1}{1-\gamma}} \left( \frac{\gamma-1}{\gamma+1} \right)^{1/2} \right]^{1-\gamma} \quad (29)$$

From Equations (28) and (29), Equation (27) now becomes:

$$\frac{M}{M'} = \left[ \frac{E}{E'} (\cos \theta)^{(E-E')} \right]^{\frac{1-\gamma}{2}} \quad (30)$$

where E is defined by Equation (13) and E' by Equation (26).

Having once constructed the flow field for a sonic nozzle from Equation (25) for a given gas, the Mach number, M, in the flow field of a nozzle with exit Mach numbers other than one can be readily determined from Equation (30). In other words, for a given gas ( $\gamma$  fixed), plots of Equation (25) and (30) are sufficient to establish the flow field Mach numbers for several nozzle exit conditions. Equations (25) and (30) are plotted in Figures 4(a) and 4(b), respectively, for  $\gamma = 1.4$ . An example calculation to demonstrate the use of these two charts is provided in the Appendix, Example 2.

In preliminary design and proposal studies, wherein various nozzle exit conditions and gases may be under investigation, plots of Equations (25) and (30) similar to that in Figures 4(a) and 4(b) for other gases should be of considerable value.

## SECTION 3

### RESULTS AND DISCUSSION

Flow field Mach numbers computed by the present approximate method are compared with available solutions by the method of characteristics for several gases and nozzles exhausting into a vacuum.

Comparisons are presented in Figures 5 and 6 for  $h/r_e < 35$ . Figure 5 shows a comparison over the entire flow field for  $M_e = 2.94$  and  $\gamma = 1.4$  (Reference 2, for a 15-degree conical nozzle);\* and, in Figure 6, the Mach number distribution along the jet centerline is compared for  $M_e = 1.0$  and  $\gamma = 1.4$  (Reference 3, for a nearly sonic orifice). Also shown in Figure 6 is the first order solution based on Equation (2).

Figures 7 and 8 show Mach number comparisons for higher values of  $h/r_e$  (between 40 and 600). The entire flow field is compared in Figure 7 for  $M_e = 3.93$  and  $\gamma = 1.26$  (Reference 4 for a 15-degree semidivergence nozzle angle). Axial Mach number comparisons are presented in Figure 8 for  $M_e = 4.0$  and  $\gamma = 1.24$  (Reference 4 for a 20-degree semidivergence nozzle angle).

Examining the axial Mach number distribution in Figures 5 through 8 (shown directly in Figures 6 and 8 and along the axis  $\theta = 0$  in Figures 5 and 7) the present method, in general, is seen to overestimate the Mach number (relative to the Mach number by the method of characteristics) at a given value of  $X/r_e$  along the axis. Inasmuch as the comparisons presented in Figures 5 and 6 are for relatively low values of  $h/r_e$ , the agreement with characteristics solutions is surprisingly good. Note, for example, in Figure 5 at  $X/r_e = 25.4$ , and in Figure 6 at  $X/r_e = 20$ , the axial Mach number computed by the present method are in error by roughly 2 percent,

---

\* In the development of this approximate method the mass flux  $\rho_e V_e A_e$  into the control surface was taken to be constant, i.e., parallel nozzle. For a conical nozzle this is still a reasonable approximation and the method should be valid for conical nozzles as well.



relative to those by the method of characteristics. At larger values of  $h/r_e$ , where the radial flow assumption is more appropriate, better agreement is evidenced. In Figure 7, at  $X/r_e = 134$ , and in Figure 8 at  $X/r_e = 500$ , the relative errors in axial Mach number are on the order of 1 percent. An examination of the axial Mach number distribution in Figure 6 reveals that the present method represents a substantial improvement over the first order solution (Reference 1). At  $X/r_e = 20$ , the relative error in axial Mach number is reduced from 16 percent (first order solution) to 2 percent by the present solution. Note also that the present solution converges toward the characteristics solution as  $X/r_e$  increases; whereas, the first order solution does not show this trend.

Normal to the jet centerline, the present method predicts the general shape of the Mach contours fairly accurately (see Figures 5 and 7). For the same constant Mach number, it is seen that the two curves (approximate and characteristics solutions) cross each other. Evidently, at the point of intersection, the agreement between the two solutions is exact. Over the entire flow field, however, no consistency is evidenced with respect to the angle  $\theta$  at which this crossover occurs.

The deviations discussed above are attributed to the assumed density profile on which the present method is based. The assumed density profile, Equation (4), does not satisfy the boundary conditions at the edge of the jet. That is, the cosine distribution of Equation (4) presumes a boundary ( $M = \infty$ ) at  $\theta = 90$  degrees, whereas, in theory, the exhaust flow from a nozzle into a vacuum can expand to an angle greater than 90 degrees, depending on the gas ratio of specific heats, and the nozzle geometry. Better correlation with the method of characteristics should be realized by considering the flow past 90 degrees. Evidently, a density distribution other than the present cosine function must be assumed.

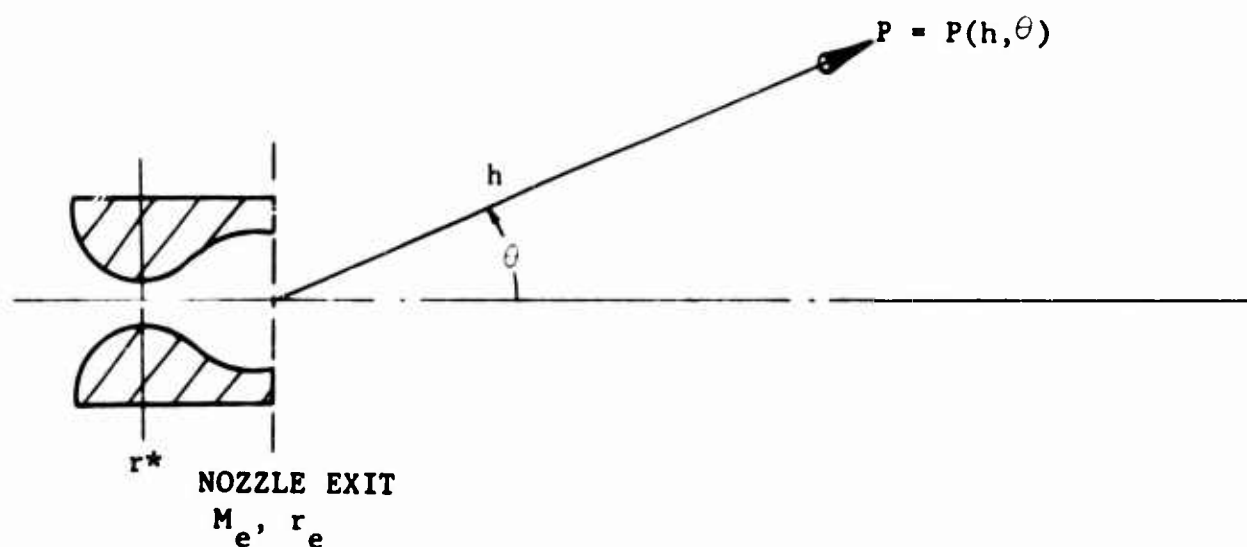
No general criteria, applicable for all gases and nozzle geometries, has been established with regard to the lower limit ( $\frac{h}{r_e}$ ) of applicability for the present method. However, an examination of several theoretical streamline patterns for nozzles exhausting into a vacuum (References 2 and 5) has indicated that for  $\gamma = 1.4$  and  $M_e \geq 3$ , the lower limit may be taken as  $h/r_e = 10$ .

The present approximate method can be extended to estimate Mach number contours for a rocket exhausting into a near vacuum environment (such as in a vacuum chamber). Whereas the flow field in a vacuum is shock free, the flow behind a rocket exhausting into a finite pressure region (at rest) is characterized by a curved shock which closely follows the jet boundary and eventually returns to the jet axis as a normal shock further downstream of the nozzle exit. The adjustment of flow to the ambient pressure occurs in the outer region between the shock and jet boundary. Interior of the shock, the flow is unaffected by the ambient pressure and is identical to the corresponding portion of a vacuum jet flow field having the same  $M_e$  and  $\gamma$ .

## REFERENCES

1. Roberts, Leonard, "The Action of a Hypersonic Jet on a Dust Layer," IAS Paper No. 63-50, January 1963.
2. Eastman, D. W., and Len Radtke, "Two Dimensional or Axially Symmetric Real Gas Flows by the Method of Characteristics, Part III: A Summary of Results from the IBM 7090 Program for Calculating the Flow Field of a Supersonic Jet," Boeing Company, Report D2-1 0599, November 1962.
3. Owen, P. L., and Thornhill, C. K., "The Flow in an Axially Symmetric Supersonic Jet from a Nearly Sonic Orifice into a Vacuum," Armament Research Establishment, Report No. 30/48, Fort Halstead, Kentucky, September 1948.
4. J. A. Hitz, Space Technology Laboratory, Private Communication.
5. Yoshihara, Hideo, "Rocket Exhaust Impingement on a Ground Surface," Journal of Fluid Mechanics, Vol. 15, Part 1, January 1963, p.p. 65-73.

APPENDIX  
EXAMPLE CALCULATIONS



The present method can be utilized to determine properties at the point  $P$  in the flow of a nozzle exhausting into a vacuum. The method is applicable for  $h/r_e \gg 1$ . For a given gas specific heat ratio ( $\gamma$ ), nozzle dimension ( $r_e$ ), and either  $(A_e/A^*)$  or  $M_e$ , properties at the point  $P$  can be determined by either of the following two methods:

- (1) The basic solution derived from continuity and momentum considerations: Equation (24) can be solved directly for the Mach number.
- (2) The generalized solution based on a sonic nozzle flow field. Combined plots of Equations (25) and (30) provide a rapid means for calculating the flow field behind a nozzle having exit Mach numbers other than one.

Example calculations are presented for  $\gamma = 1.4$ . In Example 1, the local Mach number at the point  $P$  is determined directly from Equation (24). The same problem is solved in Example 2 using the generalized procedure based on a sonic nozzle flow field (Equations 25 and 30).

## EXAMPLE CALCULATIONS

### Example 1 (Direct application of Equation 24)

Given:  $M_e = 3.0$ ,  $r_e = 2$  inch,  $\gamma = 1.4$

Calculate: Local Mach number,  $M$ , at the point  $h = 40$  inch,  $\theta = 30^\circ$

(a) Determine  $\frac{h}{r_e}$ ,  $E$ , and  $\frac{A_\star}{A_e}$  :

$$\frac{A_\star}{A_e} = \frac{1}{4.235} \quad \text{from NACA 1135 for } M_e = 3.0, \gamma = 1.4$$

$$\frac{h}{r_e} = \frac{40 \text{ in.}}{2 \text{ in.}} = 20$$

$$E = \frac{1 + \frac{1}{\gamma M_e^2}}{\sqrt{1 + \frac{2}{(\gamma-1)M_e^2} - \left(1 + \frac{1}{\gamma M_e^2}\right)}} \quad \text{Equation (13)}$$

$$E = \frac{1 + \frac{1}{(1.4)(3)^2}}{\sqrt{1 + \frac{2}{(1.4-1)(3)^2} - \left(1 + \frac{1}{1.4(3^2)}\right)}}$$

$$E = 6.43$$

(b) The Mach number,  $M$ , is calculated from Equation 24:

$$M = \left[ \frac{2}{\gamma-1} \left\{ \left[ \frac{E}{2} \cdot \frac{A_\star}{A_e} \left( \frac{h}{r_e} \right)^{-2} (\cos \theta)^{E-1} \left( \frac{\gamma+1}{2} \right)^{\frac{1}{1-\gamma}} \left( \frac{\gamma-1}{\gamma+1} \right)^{1/2} \right]^{1-\gamma} - 1 \right\} \right]^{1/2}$$

$$M = \left[ \frac{2}{1.4-1} \left\{ \left[ \left( \frac{6.43}{2} \cdot \frac{1}{4.235} (20)^{-2} (\cos 30^\circ)^{(6.43-1)} \left( \frac{1.4+1}{2} \right)^{\frac{1}{1-1.4}} \left( \frac{1.4-1}{1.4+1} \right)^{1/2} \right]^{(1-1.4)} - 1 \right\} \right]^{1/2}$$

$$M = 11.78$$

## EXAMPLE CALCULATIONS

Example 2 (From combined plots of Equations 25 and 30)

Given:  $M_e = 3.0$ ,  $r_e = 2$  inch,  $\gamma = 1.4$

Calculate: Local Mach number,  $M$ , at the point  $h = 40$  inch and  $\theta = 30^\circ$

(a) Determine  $\frac{A_\star}{A_e}$  and  $\frac{h}{r_\star}$  :

$$\frac{A_\star}{A_e} = \frac{1}{4.235} \quad \text{from NACA 1135 for } M_e = 3.0, \gamma = 1.4$$

$$\frac{h}{r_\star} = \frac{h}{r_e} \sqrt{\frac{A_e}{A_\star}} = \frac{40}{2} \sqrt{4.235}$$

$$\frac{h}{r_\star} = 41.2$$

(b) Find  $M'$  from Figure 3(a) (sonic nozzle flow field,  $\gamma = 1.4$ ):

For  $\frac{h}{r_\star} = 41.2$  and  $\theta = 30^\circ$ , from Figure 3(a):

$$M' = 12.75$$

(c) Find  $M/M'$  from Figure 3(b) (Mach number transformations-curves,  $\gamma = 1.4$ ):

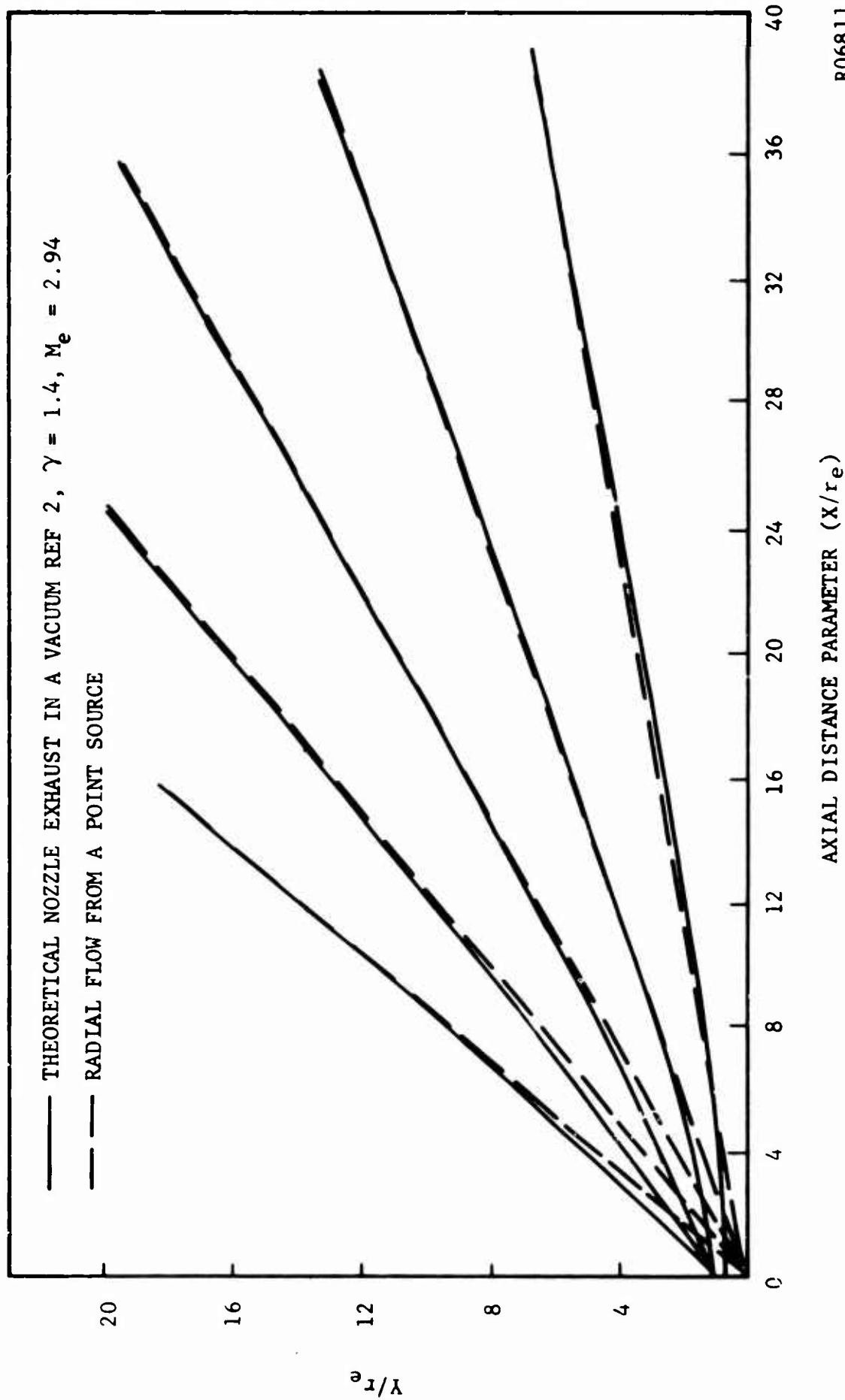
For  $M_e = 3.0$  and  $\theta = 30^\circ$

$$M/M' = 0.922$$

(d) Then:

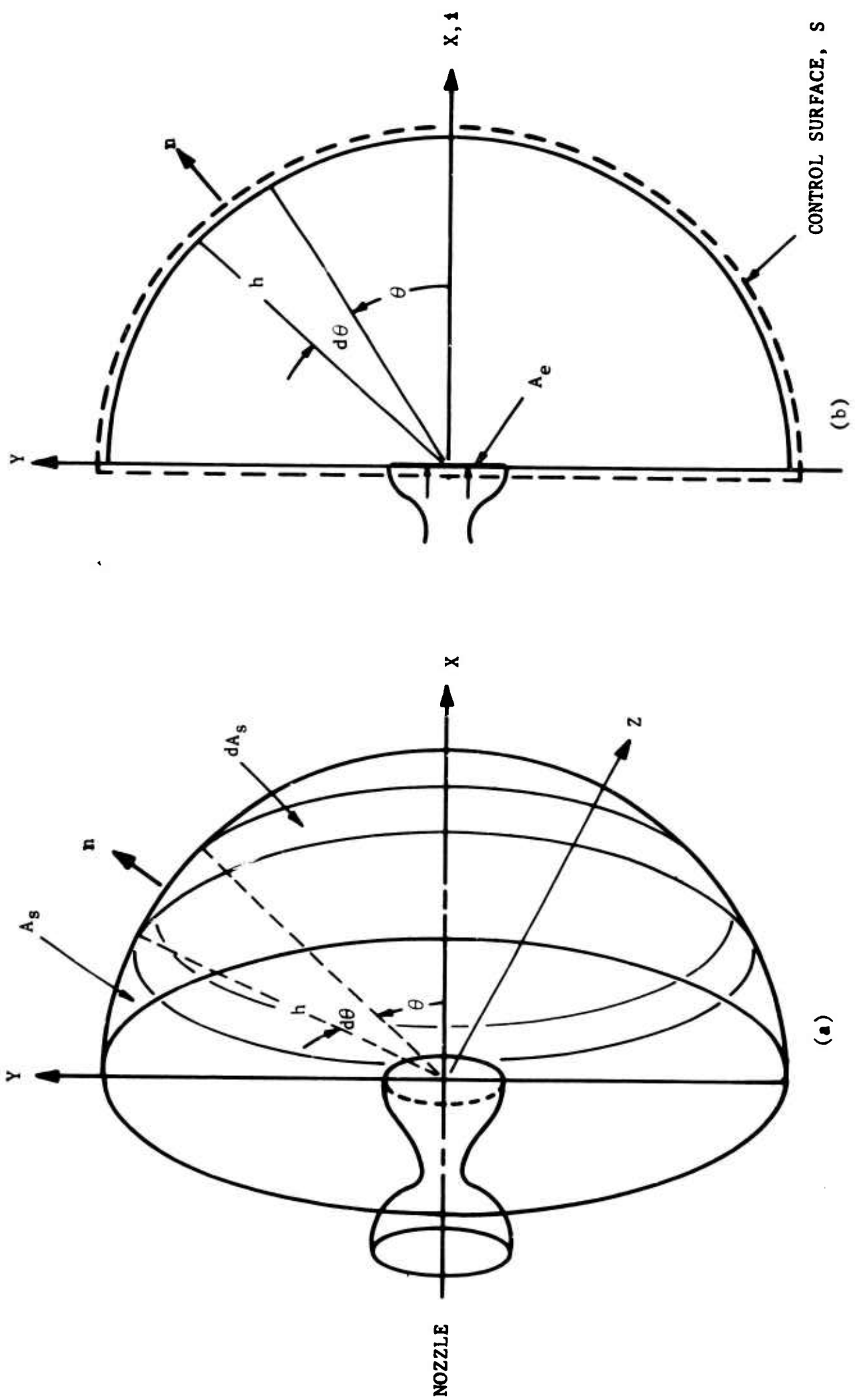
$$M = 0.922 M' = 0.922 (12.75)$$

$$M = 11.75$$



R06811

FIGURE 1. THEORETICAL STREAMLINES FOR A NOZZLE EXHAUSTING INTO A VACUUM COMPARED WITH STREAMLINES FOR RADIAL FLOW FROM A POINT SOURCE



R06814

FIGURE 2. JET GEOMETRY AND COORDINATE SYSTEM

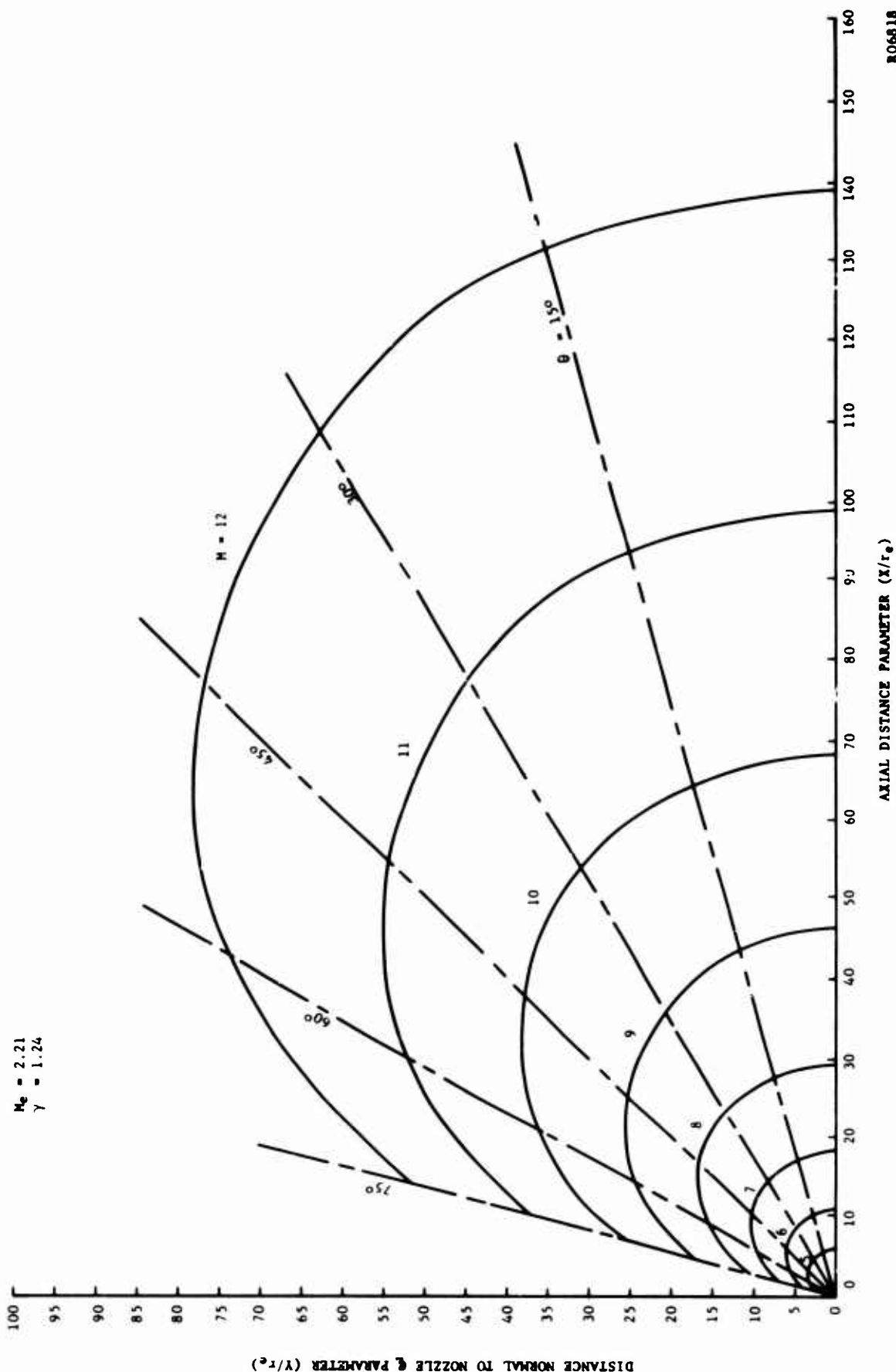
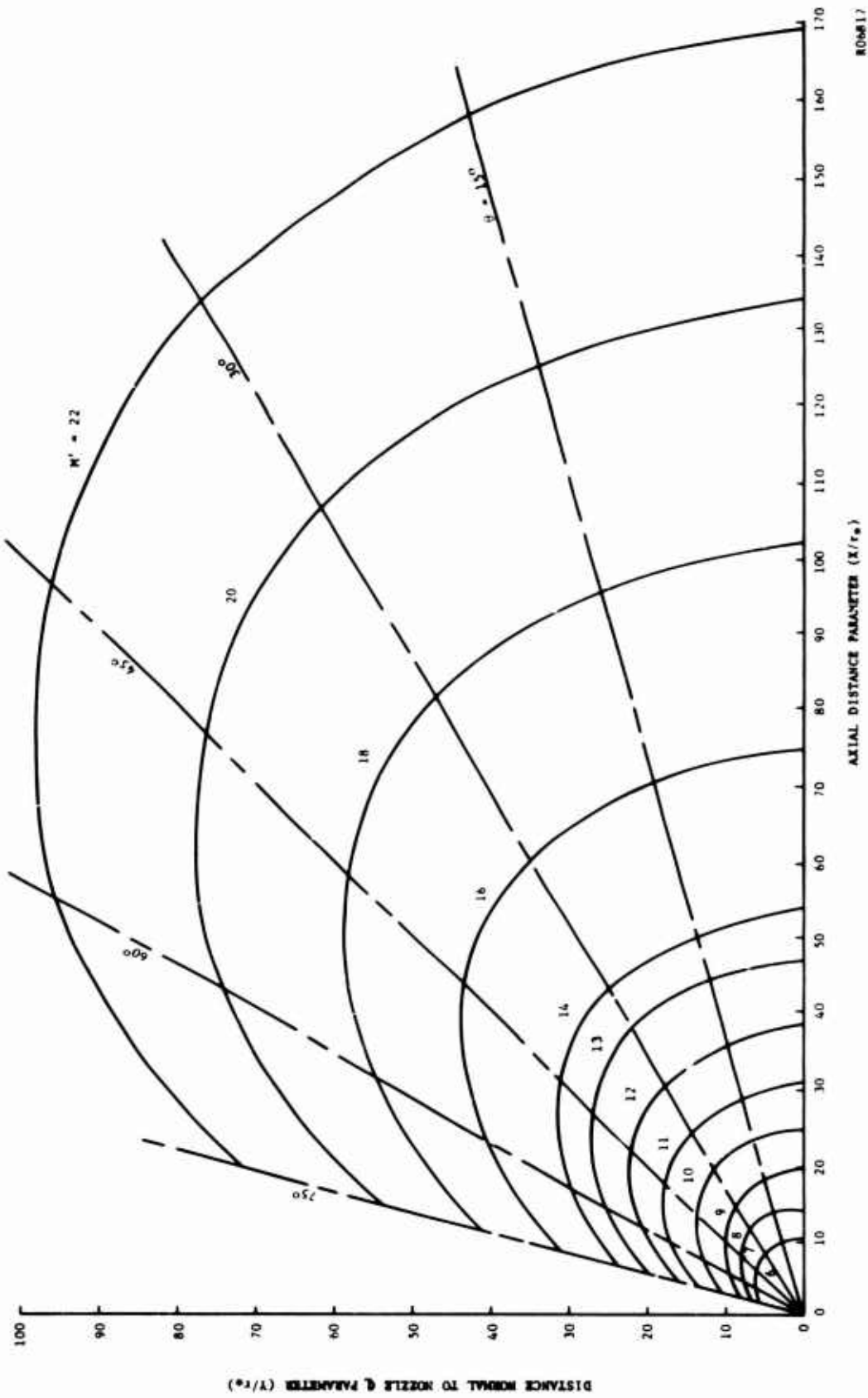


FIGURE 3. CONTOURS OF CONSTANT MACH NUMBER FOR A ROCKET EXHAUSTING INTO A VACUUM (BY PRESENT APPROXIMATE SOLUTION)





ROOM 17

FIGURE 4a. SONIC NOZZLE FLOW FIELD IN A VACUUM ( $M_e = 1.0$ ,  $\gamma = 1.4$ )

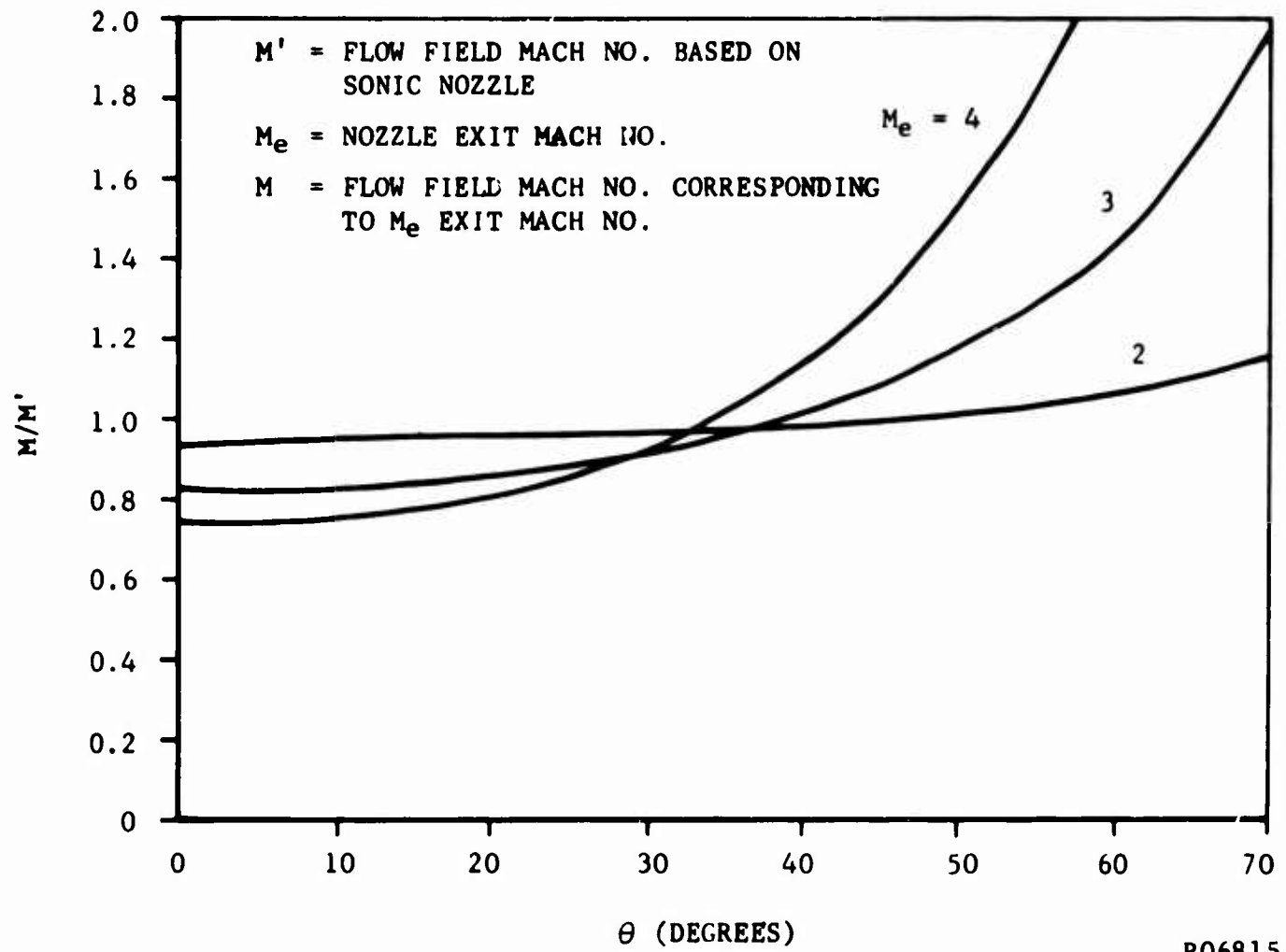
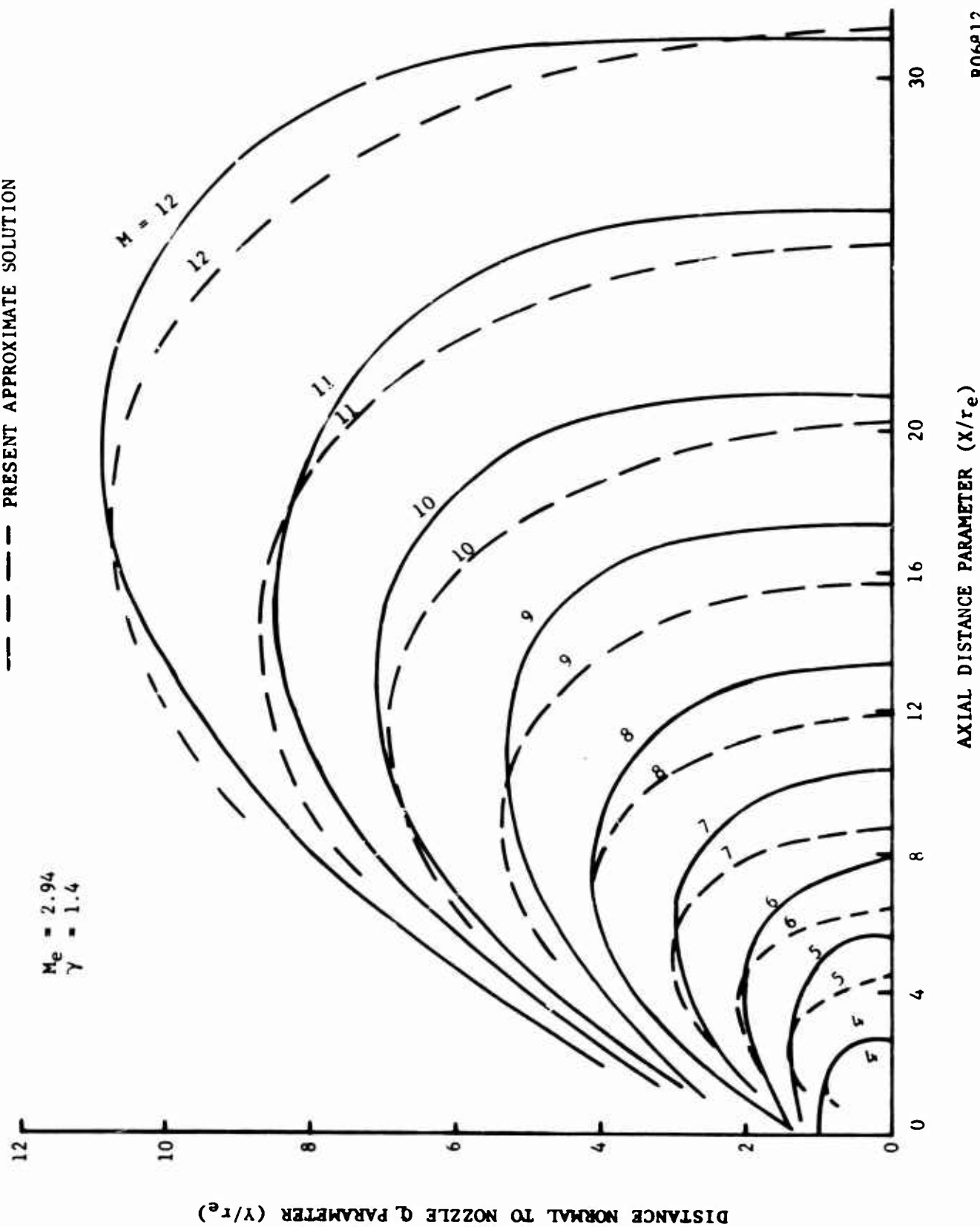


FIGURE 4b. MACH NUMBER TRANSFORMATION CURVES

———— CHARACTERISTICS SOLUTION (REF 2)

- - - - PRESENT APPROXIMATE SOLUTION



R06812

FIGURE 5. A COMPARISON OF THE APPROXIMATE AND CHARACTERISTICS SOLUTIONS FOR A ROCKET EXHAUSTING INTO A VACUUM ( $M_e = 2.94$ ,  $\gamma = 1.4$ )

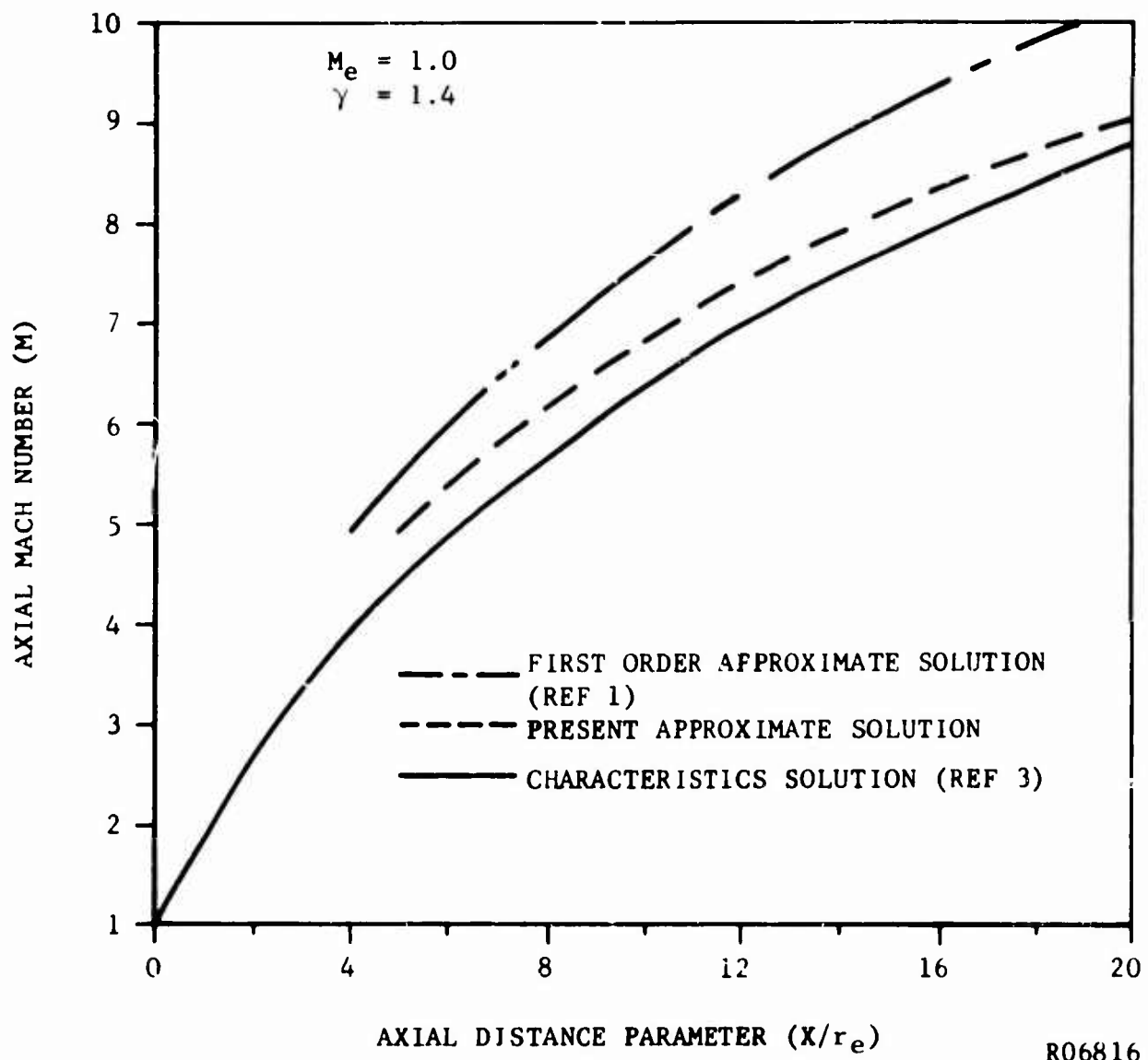
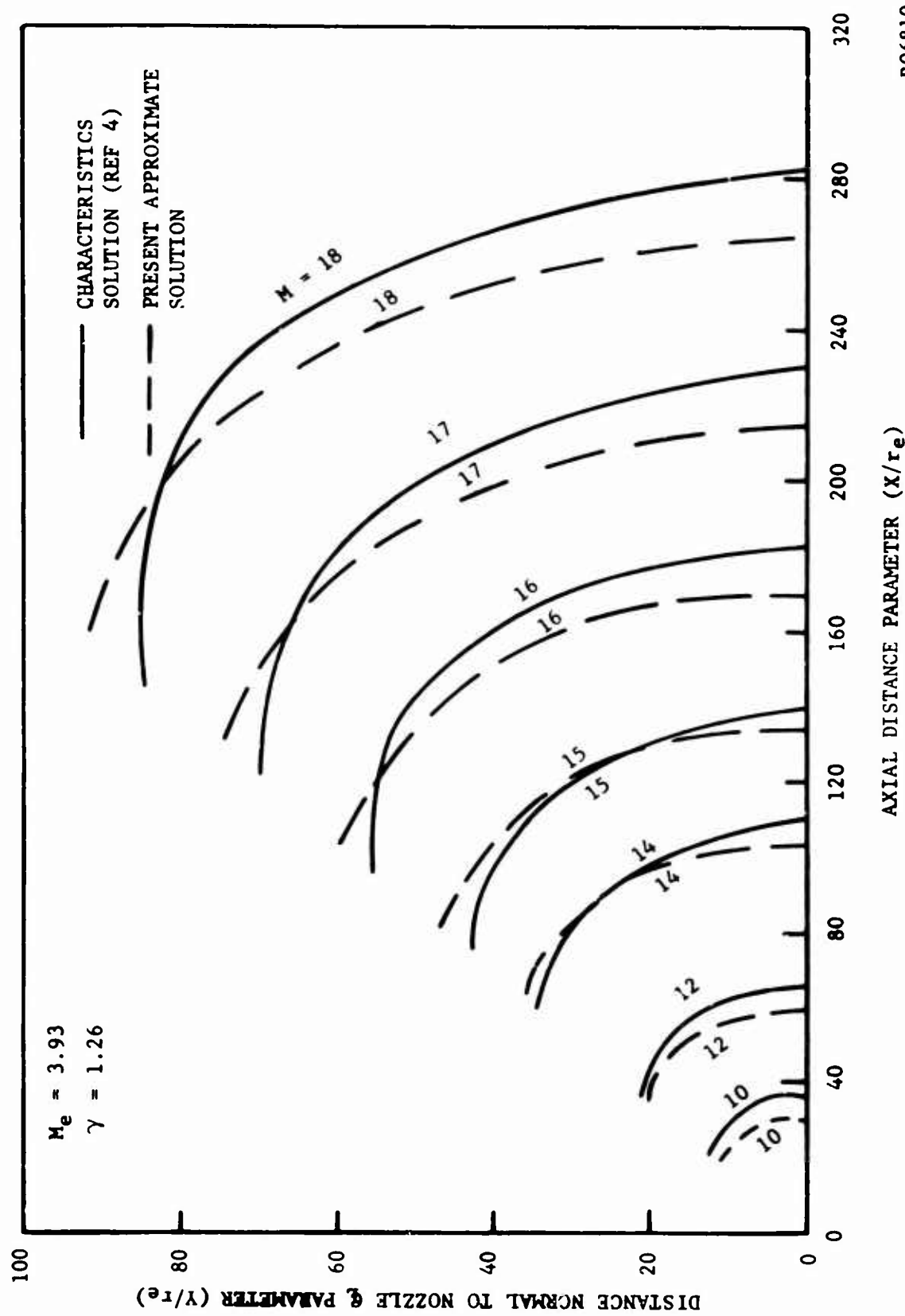


FIGURE 6. COMPARISON OF AXIAL MACH NUMBER DISTRIBUTION FOR A ROCKET EXHAUSTING INTO A VACUUM ( $M_e = 1.0$ ,  $\gamma = 1.4$ )



R06810

FIGURE 7. A COMPARISON OF THE APPROXIMATE AND CHARACTERISTICS SOLUTIONS FOR A ROCKET EXHAUSTING INTO A VACUUM ( $M_e = 3.93$ ,  $\gamma = 1.26$ )

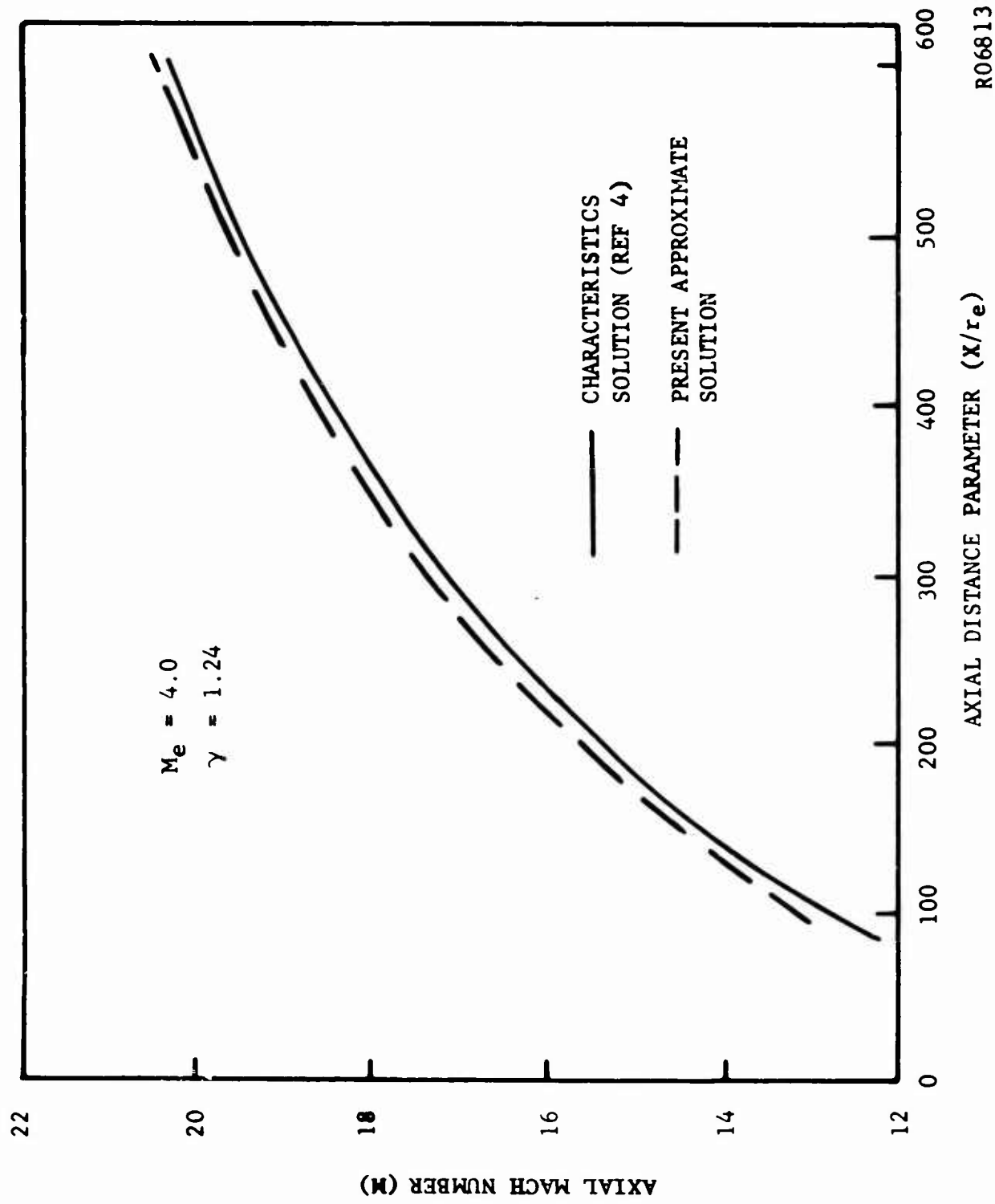


FIGURE 8. A COMPARISON OF THE APPROXIMATE AND CHARACTERISTICS SOLUTION FOR A ROCKET EXHAUSTING INTO A VACUUM ( $M_e = 4.0$ ,  $\gamma = 1.24$ )

R06813